

Chemical reactivity of ultracold polar molecules: investigation of $\text{H} + \text{HCl}$ and $\text{H} + \text{DCI}$ collisions

P.F. Weck^a and N. Balakrishnan^b

Department of Chemistry, University of Nevada Las Vegas, 4505 Maryland Parkway, Las Vegas NV 89154, USA

Received 5 June 2004

Published online 10 August 2004 – © EDP Sciences, Società Italiana di Fisica, Springer-Verlag 2004

Abstract. Quantum scattering calculations are reported for the $\text{H} + \text{HCl}(v, j = 0)$ and $\text{H} + \text{DCI}(v, j = 0)$ collisions for vibrational levels $v = 0-2$ of the diatoms. Calculations were performed for incident kinetic energies in the range $10^{-7}-10^{-1}$ eV, for total angular momentum $J = 0$ and s -wave scattering in the entrance channel of the collisions. Cross-sections and rate coefficients are characterized by resonance structures due to quasibound states associated with the formation of the $\text{H}\cdots\text{HCl}$ and $\text{H}\cdots\text{DCI}$ van der Waals complexes in the incident channel. For the $\text{H} + \text{HCl}(v, j = 0)$ collision for $v = 1, 2$, reactive scattering leading to H_2 formation is found to dominate over non-reactive vibrational quenching in the ultracold regime. Vibrational excitation of HCl from $v = 0$ to $v = 2$ increases the zero-temperature limiting rate coefficient by about 8 orders of magnitude.

PACS. 34.50.-s Scattering of atoms and molecules – 34.50.Ez Rotational and vibrational energy transfer – 34.50.Pi State-to-state scattering analyses

1 Introduction

Over the last several years, much progress has been made in cooling, trapping, and manipulating molecules at ultracold temperatures [1–6] and Bose-Einstein condensation (BEC) of diatomic molecules has recently been demonstrated [3–5]. The experimental breakthrough that led to the creation of molecular Bose-Einstein condensates starting from fermionic atoms provides unique opportunities to study the crossover regime between Bardeen-Cooper-Schrieffer-type superfluidity of momentum pairs and BEC of molecules [7–10], a topic that has been of long interest to the high temperature superconductivity community.

Collisional studies of ultracold molecules have received considerable attention in recent years [11–17] and the possibility of quantum collective effects in chemical reactions involving ultracold molecules is of particular interest [18, 19]. Polar molecules are another class of molecules that have received important attention in recent experiments. The anisotropic, long-range character of the electric dipole-dipole interactions of polar molecules also designates them as potential candidates for scalable quantum computation schemes using electric dipole moment couplings [20–23]. The techniques developed so far for creating ultracold molecules fall into three different categories, namely buffer-gas cooling of paramagnetic molecules [1, 24–26], electrostatic cooling of polar molecules [27–30] and photoassociation of ultracold

atoms [31–35]. While the first two approaches have been successful in trapping polar molecules at cold temperatures of 10–100 mK, the creation of ultracold ($T \simeq 100 \mu\text{K}$) polar neutral ground state molecules (KRb) was achieved only recently by photoassociation in a magneto-optical trap [36]. Formation of electronically excited RbCs molecules by photoassociation in a laser-cooled mixture of ^{85}Rb and ^{133}Cs atoms [37, 38] has also been reported.

Photoassociation creates molecules in highly excited vibrational levels and their lifetime is restricted by collisions leading to vibrational relaxation and/or chemical reactivity [39, 40]. The effect of vibrational excitation on quenching rate coefficients in the ultracold regime has been explored before but similar studies on chemical reactivity have not been reported. In this work, we report quantum scattering calculations of atom-diatom reactions at cold and ultracold temperatures in which the diatom is taken to be a highly polar molecule. Previous studies of ultracold chemical reactions investigated nonpolar molecules like H_2 [39], its isotopic counterparts [40, 41] or alkali metal dimers [16]. Here, we investigate the bimolecular $\text{H} + \text{HCl}$ and $\text{H} + \text{DCI}$ collisions at low and ultralow energies for which the reaction proceeds mainly by quantum tunneling of the exchanged atom through a barrier along the reaction path. As elementary steps in the $\text{H}_2 + \text{Cl}_2$ reaction system, which plays a major role in chemical kinetics and in atmospheric chemistry, the gas-phase $\text{H} + \text{HCl}$ and $\text{Cl} + \text{H}_2$ reactions and their isotopic variants have received important attention both theoretically [42–52] and experimentally [44, 53–57]. However, these kinetics studies

^a e-mail: weckp@unlv.nevada.edu

^b e-mail: naduvala@unlv.nevada.edu

and experiments have been carried out in the temperature range $195 \text{ K} \leq T \leq 3020 \text{ K}$ and no scattering calculations have been reported so far for these reactions in the cold and ultracold regimes, to our knowledge.

In this paper, we present results for state-to-state and initial-state-selected probabilities and cross-sections for both reactive and non-reactive channels of the $\text{H} + \text{HCl}(v, j = 0)$ and $\text{H} + \text{DCl}(v, j = 0)$ collisions for vibrational levels $v = 0-2$ in the ground electronic state. The presence of pronounced resonance structures due to quasi-bound states associated with van der Waals complexes in the initial channel is discussed. Finally, reaction rate coefficients for H_2 and HD formations are also presented as a function of the temperature and in the zero-temperature limit. We show that vibrational excitation of HCl and DCl dramatically increases the rate coefficients in the ultracold regime.

2 Calculations

The quantum mechanical coupled-channel hyperspherical coordinate method of Skouteris et al. [58] is used to solve the Schrödinger equation for the motion of the three nuclei on the parametric representation of the single Born-Oppenheimer potential energy surface (PES) developed by Bian and Werner (BW) [59]. The small effect of the fine-structure observed in similar reactions [52,60,61] supports our choice to neglect the spin-orbit splitting in the $\text{Cl}(^2\text{P})$ atom. Although the accuracy of this potential energy surface for ultracold collision studies is questionable, based on our experience we believe that major findings of our study will not be affected if a more accurate ClH_2 potential surface is used.

Scattering calculations were performed for a total molecular angular momentum $J = 0$ and s -wave scattering in the incident channel of the $\text{H} + \text{HCl}(v, j = 0)$ and $\text{H} + \text{DCl}(v, j = 0)$ collisions for vibrational states $v = 0-2$. We note that in the case of weak trapping potentials, which are expected to allow long decoherence times in 1D trap arrays of quantum computers [23], only s -wave scattering is expected to play a significant role [62]. Because at very low kinetic and internal energies these reactions proceed mainly by quantum tunneling, the resulting reaction probabilities are very small and particular attention must be paid to convergence. Extensive convergence tests of the initial-state-selected and state-to-state reaction probabilities have been carried out, with respect to the number of rovibrational levels included in the basis set, j_{max} , the maximum value of the hyperradius, ρ_{max} , and the step size for the log derivative propagation, $\Delta\rho$. Figure 1 shows the total reaction probability for H_2 formation in $\text{H} + \text{HCl}(v = 0; j = 0)$ collisions as a function of the incident kinetic energy for different values of ρ_{max} and $\Delta\rho$. Convergence of the total reaction probability with an accuracy of the order of 10^{-10} was obtained with $\rho_{\text{max}} = 25.0 \text{ a.u.}$ and $\Delta\rho = 0.005 \text{ a.u.}$ for kinetic energies in the range $10^{-5}-10^{-3} \text{ eV}$. Using these values of ρ_{max} and $\Delta\rho$, a more stringent convergence test consisted in the analysis of the product rota-

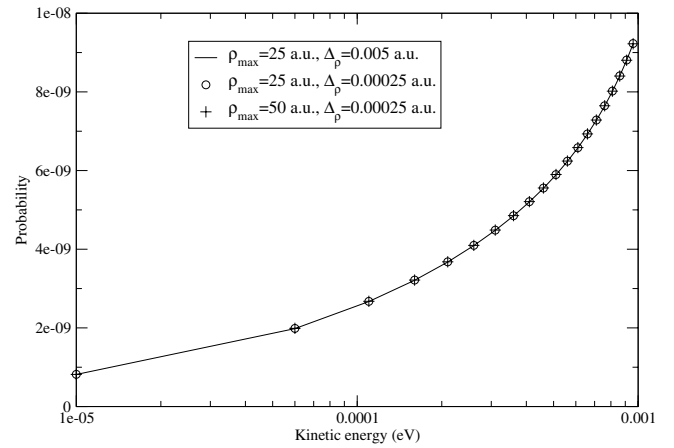


Fig. 1. Reaction probability for H_2 formation in $\text{H} + \text{HCl}(v = 0, j = 0)$ collisions as a function of the incident kinetic energy for different values of ρ_{max} and $\Delta\rho$.

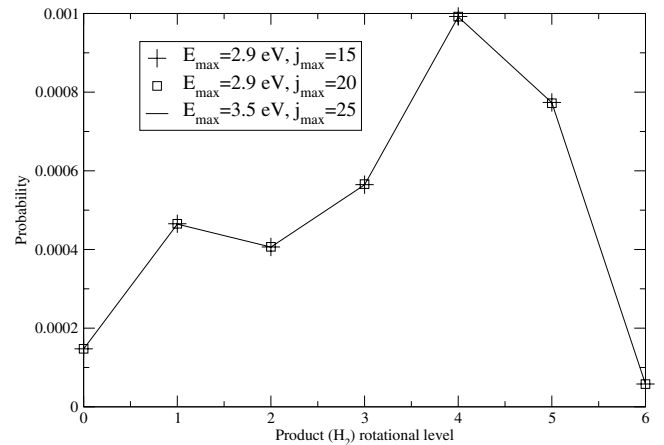


Fig. 2. State-to-state reaction probability for $\text{H}_2(v' = 0, j')$ formation as a function of j' in $\text{H} + \text{HCl}(v = 1, j = 0)$ collisions, for different values of E_{max} and j_{max} , at an incident kinetic energy of 10^{-3} eV , $\rho_{\text{max}} = 25.0 \text{ a.u.}$, and $\Delta\rho = 0.005 \text{ a.u.}$

tional (j') distribution. For an incident kinetic energy of 10^{-3} eV , convergence of the state-to-state probability for $\text{H} + \text{HCl}(v = 0, 1; j = 0)$ and $\text{H} + \text{DCl}(v = 0, 1; j = 0)$ was achieved to within 10^{-10} using $j_{\text{max}} = 15$ and a cutoff internal energy $E_{\text{max}} = 2.9 \text{ eV}$ in any channel. The resulting basis sets for HCl and DCl collisions consisted of 376 and 456 basis functions, respectively. Figure 2 illustrates the convergence of the state-to-state reaction probability with respect to j_{max} and E_{max} for $\text{H}_2(v' = 0, j')$ formation in $\text{H} + \text{HCl}(v = 1, j = 0)$ collisions, for an incident kinetic energy of 10^{-3} eV , $\rho_{\text{max}} = 25.0 \text{ a.u.}$, and $\Delta\rho = 0.005 \text{ a.u.}$ Convergence of the state-to-state probabilities for the $\text{H} + \text{HCl}(v = 2; j = 0)$ and $\text{H} + \text{DCl}(v = 2; j = 0)$ collisions was achieved using larger basis sets of 721 and 891 basis functions, respectively, corresponding to $j_{\text{max}} = 25$ and $E_{\text{max}} = 3.5 \text{ eV}$. On the basis of these convergence tests, values of $j_{\text{max}} = 15$ and $E_{\text{max}} = 2.9 \text{ eV}$ for $v = 0, 1$ and of $j_{\text{max}} = 25$ and $E_{\text{max}} = 3.5 \text{ eV}$ for $v = 2$ were adopted for the calculations reported hereafter.

3 Results and discussion

The cross-sections for H_2 and HCl formation and for non-reactive scattering in $\text{H} + \text{HCl}(v, j = 0)$ collisions are shown in Figure 3, for $v = 0-2$, for incident kinetic energy in the range $10^{-7}-10^{-1}$ eV. For HCl molecules initially in their ground vibrational state, the reaction proceeds mainly by quantum tunneling through the barrier, yielding small values for the cross-sections. We note that for the $v = 0, j = 0$ initial state nonreactive channels are open only for incident kinetic energy larger than 2.585×10^{-3} eV, corresponding to the energy value for rotational excitation to the first excited level $j = 1$ of the ground vibrational state. The sharp rise in the cross-section for nonreactive scattering at energies above 2.585×10^{-3} eV is due to rotational excitation to the $j = 1$ level. In the zero-temperature limit, the cross-section for the abstraction reaction leading to H_2 formation is about 9 orders of magnitude larger than the exchange mechanism leading to HCl formation, consistent with the fact that the transmission coefficient for tunneling of the H atom through a finite potential barrier is larger than for heavier atoms like chlorine [63]. As v increases and the barrier height decreases, the H_2/HCl product branching ratio decreases, with values differing by 3 orders of magnitude for $v = 1$, and 2 orders of magnitude for $v = 2$ at an incident kinetic energy of 10^{-7} eV. For energies below 10^{-4} eV, cross-sections reach the Wigner regime [64] where they vary inversely as the velocity and their ratios become constant. For the $v = 0, j = 0$ case, the hydrogen exchange process is indistinguishable from elastic scattering and the cross-section attains a constant value in the Wigner limit as expected for elastic scattering. For kinetic energies larger than 10^{-3} eV, pronounced resonance structures appear in the cross-sections due to quasibound states associated with the formation of the $\text{H} \cdots \text{HCl}$ van der Waals complex in the initial channel, as reported previously for different molecular systems [65–68]. Figure 4 shows cross-sections for HD and HCl formation as well as nonreactive scattering in $\text{H} + \text{DCl}(v, j = 0)$ collisions as functions of the incident kinetic energy. Cross-sections are presented only for the first two vibrationally excited states $v = 1$ and 2 due to the negligible values obtained for the $v = 0$ level of DCl . While nonreactive cross-sections have similar magnitude as for $\text{H} + \text{HCl}(v, j = 0)$ collisions, reactive cross-sections are several orders of magnitude smaller for the deuterated reaction, the difference being attributed to the less efficient tunneling of the heavier D atom.

State-to-state reaction probabilities as a function of the product rotational quantum number j' are represented in Figure 5 for the ground vibrational state of the H_2 and HD fragments in $\text{H} + \text{HCl}(v = 1, j = 0)$ and $\text{H} + \text{DCl}(v = 1, j = 0)$ collisions, respectively. For a fixed incident kinetic energy of 10^{-5} eV, 7 rotational levels are energetically accessible in the diatomic products of both reactions. High- j channels of H_2 are preferentially populated even though lower-lying rotational states are open. The probability for H_2 formation in its ground vibrational state peaks at $j' = 4$, corresponding to an exoergicity of 0.2379 eV = 5.487 kcal/mol for the abstraction reaction.

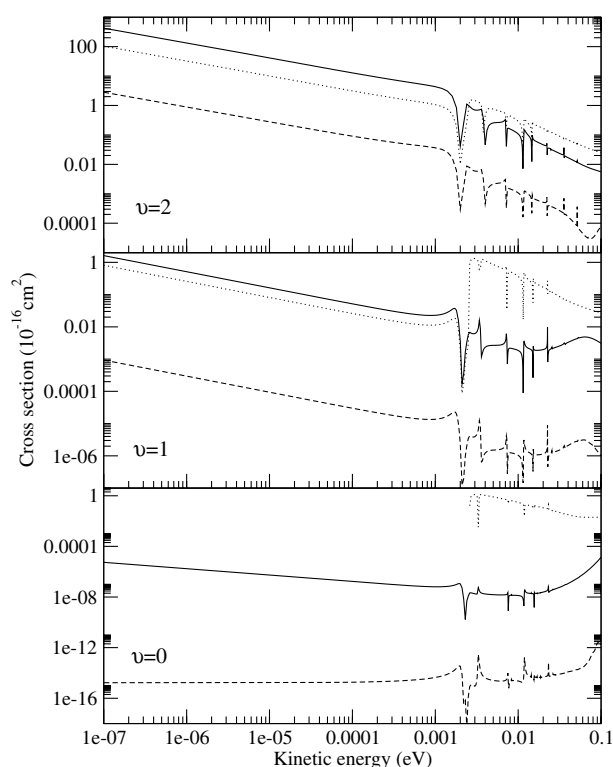


Fig. 3. Cross-sections for H_2 and HCl formation and nonreactive scattering in $\text{H} + \text{HCl}(v, j = 0)$ collisions, for $v = 0-2$, as a function of the incident kinetic energy. Dotted curve: nonreactive scattering; dashed curve: reactive HCl product channel; solid curve: H_2 product channel.

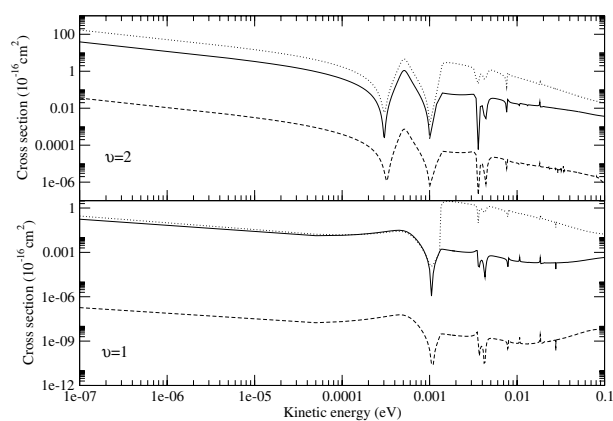


Fig. 4. Cross-sections for HD and HCl formation and nonreactive scattering in $\text{H} + \text{DCl}(v, j = 0)$ collisions, for $v = 1, 2$, as a function of the incident kinetic energy. Dotted curve: nonreactive scattering; dashed curve: reactive HCl product channel; solid curve: HD product channel.

In the case of $\text{HD}(v' = 0)$ formation, the maximum energy released by this reaction is 0.2354 eV = 5.429 kcal/mol, for $j' = 2$, with a significantly reduced probability than for the H_2 case.

Figure 6 displays the reaction rate coefficients defined as the product of the cross-section and the relative velocity for H_2 and HD formation for the $\text{H} + \text{HCl}(v, j = 0)$ and

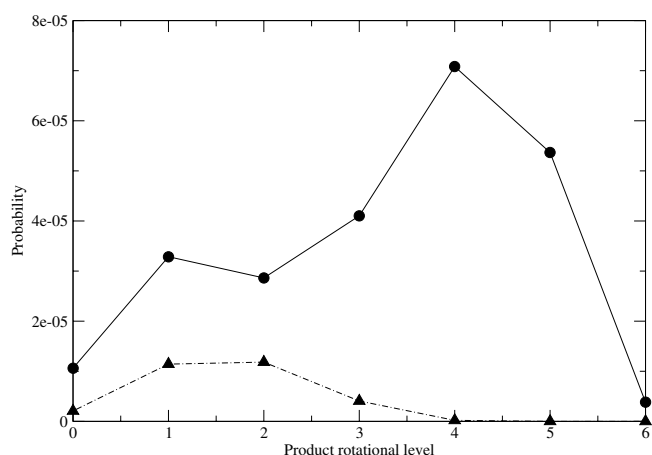


Fig. 5. Comparison of the state-to-state reaction probabilities for $\text{H}_2(v' = 0, j')$ (solid curve) and $\text{HD}(v' = 0, j')$ (dot-dashed curve) formation in $\text{H} + \text{HCl}(v = 1, j = 0)$ and $\text{H} + \text{DCl}(v = 1, j = 0)$ collisions, respectively. The probability is represented as a function of the product rotational number j' for a fixed incident kinetic energy of 10^{-5} eV.

$\text{H} + \text{DCl}(v, j = 0)$ reactions, respectively, for $v = 0-2$, as a function of the temperature. The Wigner regime, for which the rate coefficients become constant, is attained for temperatures below 1 K for H_2 formation, and below 10^{-3} K for the HD product. For $v = 1$ and 2, the rate coefficients for H_2 production is an order of magnitude larger than for HD at cold and ultracold temperatures. However, for $v = 1$ the rate coefficient for HD formation becomes slightly larger than for H_2 in the tunneling region of the $\text{H} + \text{DCl}$ reaction, i.e. around $T = 5$ K. In the zero-temperature limit, the rate coefficients calculated for H_2 and HD formation, respectively, are $1.9 \times 10^{-11} \text{ cm}^3 \text{ s}^{-1}$ and $1.7 \times 10^{-12} \text{ cm}^3 \text{ s}^{-1}$ for $v = 2$, $7.2 \times 10^{-14} \text{ cm}^3 \text{ s}^{-1}$ and $7.8 \times 10^{-15} \text{ cm}^3 \text{ s}^{-1}$ for $v = 1$, and $2.4 \times 10^{-19} \text{ cm}^3 \text{ s}^{-1}$ for H_2 with $v = 0$.

4 Conclusion

State-to-state and initial-state-selected cross-sections have been calculated using fully quantum mechanical techniques for both reactive and non-reactive channels of the $\text{H} + \text{HCl}(v, j = 0)$ and $\text{H} + \text{DCl}(v, j = 0)$ collisions, for $v = 0-2$. Resonance structures due to quasibound states of the $\text{H} \cdots \text{HCl}$ and $\text{H} \cdots \text{DCl}$ van der Waals wells in the entrance valley appear in energy dependence of the cross-sections. Our results also indicate that H_2 formation is the predominant process of $\text{H} + \text{HCl}$ collisions at cold and ultracold temperatures, while for $\text{H} + \text{DCl}$ non-reactive scattering is more favorable in this regime. We find that, for both $\text{H} + \text{HCl}$ and $\text{H} + \text{DCl}$ collisions, vibrational excitation dramatically enhances the zero-temperature limiting value of the rate coefficients. The effect of vibrational excitation is found to be comparable for reactive and non-reactive channels in the ultracold limit.

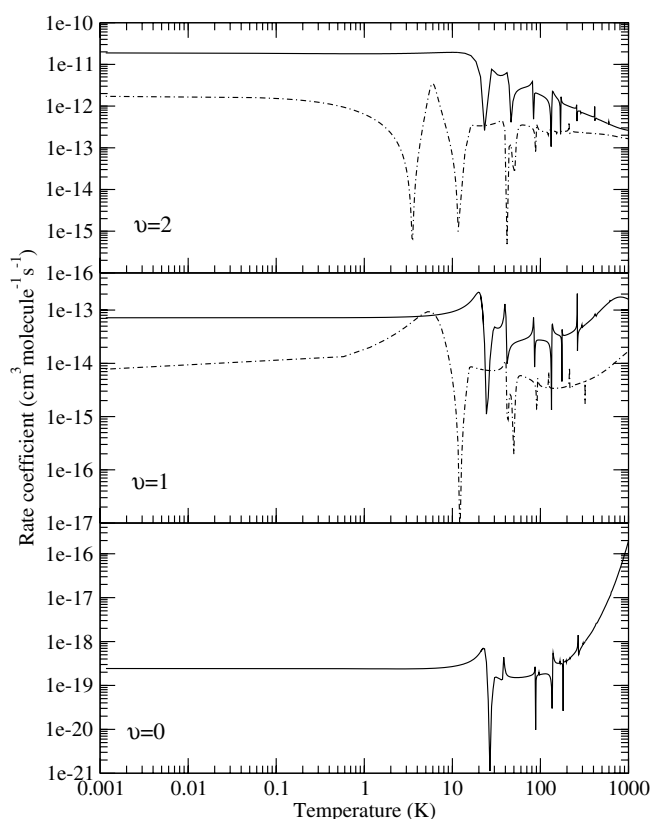


Fig. 6. Reaction rate coefficients for H_2 and HD formation for the $\text{H} + \text{HCl}(v, j = 0)$ (solid curve) and $\text{H} + \text{DCl}(v, j = 0)$ (dot-dashed curve) reactions, for $v = 0-2$, as a function of the temperature.

This work was supported by NSF grant PHYS-0245019, the Research Corporation and by the United States-Israel Binational Science Foundation.

References

1. J.D. Weinstein, R. deCarvalho, T. Guillet, B. Friedrich, J.M. Doyle, *Nature* **395**, 148 (1998)
2. H.L. Bethlem, G. Berden, F.M.H. Crompvoets, R.T. Jongma, A.J. van Roij, G. Meijer, *Nature* **406**, 491 (2000)
3. S. Jochim et al., *Science* **302**, 2101 (2003)
4. M. Greiner, C.A. Regal, D.S. Jin, *Nature* **426**, 537 (2003)
5. M.W. Zwierlein, C.A. Stan, C.H. Schunk, S.M. Raupach, S. Gupta, Z. Hafzibabic, W. Ketterle, *Phys. Rev. Lett.* **91**, 250401 (2003)
6. J. Cubizolles, T. Bourdel, S.J. Kokkelmans, G.V. Shlyapnikov, C. Salomon, *Phys. Rev. Lett.* **91**, 240401 (2003)
7. E. Timmermans, K. Furuya, P.W. Milonni, A.K. Kerman, *Phys. Lett. A* **285**, 228 (2001)
8. C.A. Regal, M. Greiner, D.S. Jin, *Phys. Rev. Lett.* **92**, 040403 (2004)
9. M. Bartenstein, A. Altmeyer, S. Riedl, S. Jochim, C. Chin, J. Hecker Denschlag, R. Grimm, *Phys. Rev. Lett.* **92**, 120401 (2004)
10. T. Bourdel et al., eprint [arXiv:cond-mat/0403091](https://arxiv.org/abs/cond-mat/0403091) (2004)

11. N. Balakrishnan, R.C. Forrey, A. Dalgarno, *Phys. Rev. Lett.* **80**, 3224 (1998)
12. N. Balakrishnan, A. Dalgarno, R.C. Forrey, *J. Chem. Phys.* **113**, 621 (2000)
13. N. Balakrishnan, G.C. Groenenboom, R.V. Krems, A. Dalgarno, *J. Chem. Phys.* **118**, 7386 (2003)
14. T. Stoecklin, A. Voronin, J.C. Rayez, *Phys. Rev. A* **68**, 032716 (2003)
15. K. Tilford, M. Hoster, P.M. Florian, R.C. Forrey, *Phys. Rev. A* **69**, 052705 (2004)
16. P. Soldán, M.T. Cvitas, J.M. Hutson, P. Honvault, J.M. Launay, *Phys. Rev. Lett.* **89**, 153201 (2002)
17. A. Volpi, J.L. Bohn, *J. Chem. Phys.* **119**, 866 (2003)
18. D.J. Heinzen, R. Wynar, P.D. Drummond, K.V. Kheruntsyan, *Phys. Rev. Lett.* **84**, 5029 (2000)
19. J.J. Hope, M.K. Olsen, *Phys. Rev. Lett.* **86**, 3220 (2001)
20. A. Barenco, D. Deutsch, A. Ekert, R. Jozsa, *Phys. Rev. Lett.* **74**, 4083 (1995)
21. G.K. Brennen, C.M. Caves, P.S. Jessen, I.H. Deutsch, *Phys. Rev. Lett.* **82**, 1060 (1999)
22. P. Platzman, M. Dykman, *Science* **284**, 1967 (1999)
23. D. DeMille, *Phys. Rev. Lett.* **88**, 067901 (2002)
24. J.M. Doyle, B. Friedrich, J. Kim, D. Patterson, *Phys. Rev. A* **52**, R2515 (1995)
25. R. deCarvalho, J.M. Doyle, B. Friedrich, T. Guillet, D. Patterson, J.D. Weinstein, *Eur. Phys. J. D* **7**, 289 (1999)
26. B. Friedrich, J.D. Weinstein, R. deCarvalho, J.M. Doyle, *J. Chem. Phys.* **110**, 2376 (1999)
27. J.A. Maddi, T.P. Dinneen, H. Gould, *Phys. Rev. A* **60**, 3882 (1999)
28. F.M. Cropvoets, H.L. Bethlem, R.T. Jongma, G. Meijer, *Nature* **411**, 174 (2001)
29. H.L. Bethlem, A.J. van Roij, R.T. Jongma, G. Meijer, *Phys. Rev. Lett.* **88**, 13003 (2002)
30. S.Y. van de Meerakker, R.T. Jongma, G. Meijer, *Phys. Rev. A* **64**, R041401 (2002)
31. A. Fioretti, D. Comparat, A. Crubellier, O. Dulieu, F. Masnou-Seeuws, P. Pillet, *Phys. Rev. Lett.* **80**, 4402 (1998)
32. T. Takekoshi, B.M. Patterson, R.J. Kinze, *Phys. Rev. Lett.* **81**, 5105 (1998)
33. A.N. Nikolov, J.R. Ensher, E.E. Eyler, H. Wang, W.C. Stwalley, P.L. Gould, *Phys. Rev. Lett.* **84**, 246 (2000)
34. C. Gabbanini, A. Fioretti, A. Lucchesini, S. Gozzini, M. Mazzoni, *Phys. Rev. Lett.* **84**, 2814 (2000)
35. M. Pichler, W.C. Stwalley, R. Beuc, G. Pichler, *Phys. Rev. A* **69**, 013403 (2004)
36. M.W. Mancini, G.D. Telles, A.R.L. Caires, V.S. Bagnato, L.G. Marcassa, *Phys. Rev. Lett.* **92**, 133203 (2004)
37. A.J. Kerman, J.M. Sage, S. Sainis, T. Bergeman, D. DeMille, *Phys. Rev. Lett.* **92**, 033004 (2004)
38. A.J. Kerman, J.M. Sage, S. Sainis, T. Bergeman, D. DeMille, *Phys. Rev. Lett.* **92**, 153001 (2004)
39. N. Balakrishnan, A. Dalgarno, *Chem. Phys. Lett.* **341**, 652 (2001)
40. E. Bodo, F.A. Gianturco, A. Dalgarno, *J. Chem. Phys.* **116**, 9222 (2002)
41. N. Balakrishnan, A. Dalgarno, *J. Phys. Chem. A* **107**, 7101 (2003)
42. S.E. Branchett, S.B. Padkjaer, J.-M. Launay, *Chem. Phys. Lett.* **208**, 523 (1993)
43. F.J. Aoiz, V.J. Herrero, V. Sáez Rábanos, I. Tanarro, E. Verdasco, *Chem. Phys. Lett.* **306**, 179 (1999)
44. F.J. Aoiz et al., *J. Phys. Chem. A* **104**, 10452 (2000)
45. A. Hanf, A. Läuiter, D. Suresh, H.-R. Volpp, J. Wolfrum, *Chem. Phys. Lett.* **340**, 71 (2001)
46. M.-D. Chen, K.-L. Han, N.-Q. Lou, *Chem. Phys.* **283**, 463 (2002)
47. L. Yao, K.-L. Han, H.-S. Song, D.-H. Zhang, *J. Phys. Chem. A* **107**, 2781 (2003)
48. F.J. Aoiz, L. Bañares, *Chem. Phys. Lett.* **247**, 232 (1995)
49. U. Manthe, W. Bian, H.-J. Werner, *Chem. Phys. Lett.* **313**, 647 (1999)
50. C. Shen, T. Wu, G. Ju, W. Bian, *Chem. Phys.* **272**, 61 (2001)
51. D. Skouteris, A. Laganá, G. Capecchi, H.-J. Werner, *Int. J. Quant. Chem.* **96**, 562 (2002)
52. C. Balucani et al., *Phys. Rev. Lett.* **91**, 013201 (2003)
53. P.M. Aker, G.J. Germann, J.J. Valentini, *J. Phys. Chem.* **90**, 4795 (1989)
54. P.M. Aker, G.J. Germann, K.D. Tabor, J.J. Valentini, *J. Phys. Chem.* **90**, 4809 (1989)
55. V.J. Barclay, B.A. Collings, J.C. Polanyi, J.H. Wang, *J. Phys. Chem.* **95**, 2921 (1991)
56. R.A. Brownsword, C. Kappel, P. Schmiechen, H.P. Upadhyaya, H.-R. Volpp, *Chem. Phys. Lett.* **289**, 241 (1998)
57. C.A. Taatjes, *Chem. Phys. Lett.* **306**, 33 (1999)
58. D. Skouteris, J.F. Castillo, D.E. Manolopoulos, *Comput. Phys. Commun.* **133**, 128 (2000)
59. W. Bian, H.-J. Werner, *J. Chem. Phys.* **112**, 220 (2000)
60. M.H. Alexander, D.E. Manolopoulos, H.-J. Werner, *J. Chem. Phys.* **113**, 5710 (1998)
61. M.H. Alexander, D.E. Manolopoulos, H.-J. Werner, *J. Chem. Phys.* **113**, 11084 (2000)
62. M. Kajita, *Eur. Phys. J. D* **23**, 337 (2003)
63. N. Balakrishnan, A. Dalgarno, *J. Phys. Chem. A* **107**, 7101 (2003)
64. E.P. Wigner, *Phys. Rev.* **73**, 1002 (1948)
65. G.A. Parker, R.T. Pack, A. Laganá, *Chem. Phys. Lett.* **202**, 75 (1993)
66. S.C. Althorpe, D.J. Kouri, D.K. Hoffman, *Phys. Chem. A* **102**, 9494 (1998)
67. M. Lara, A. Aguado, M. Paniagua, O.J. Roncero, *J. Chem. Phys.* **113**, 1781 (2000)
68. L. Wei, A.W. Jasper, D.G. Truhlar, *J. Phys. Chem. A* **107**, 7236 (2003)